

Rapid report

## Morphology of fast-tumbling bicelles: a small angle neutron scattering and NMR study

Paul A. Luchette <sup>a</sup>, Tatiana N. Vetman <sup>a</sup>, R. Scott Prosser <sup>a,\*</sup>, Robert E.W. Hancock <sup>b</sup>,  
Mu-Ping Nieh <sup>c</sup>, Charles J. Glinka <sup>c</sup>, Susan Krueger <sup>c</sup>, John Katsaras <sup>d</sup>

<sup>a</sup> Department of Chemistry, Kent State University, Kent, OH 44242, USA

<sup>b</sup> Department of Microbiology and Immunology, No. 300-6174 University Boulevard, University of British Columbia, Vancouver, BC, Canada V6T 1Z3

<sup>c</sup> Materials Science and Engineering Laboratory, National Institute of Standards and Technology, Gaithersburg, MD 20899, USA

<sup>d</sup> National Research Council, Steacie Institute for Molecular Sciences, Neutron Program for Material Research, Chalk River Laboratories, Chalk River, ON, Canada

Received 21 March 2001; accepted 15 May 2001

### Abstract

Bilayered micelles, or bicelles, which consist of a mixture of long- and short-chain phospholipids, are a popular model membrane system. Depending on composition, concentration, and temperature, bicelle mixtures may adopt an isotropic phase or form an aligned phase in magnetic fields. Well-resolved <sup>1</sup>H NMR spectra are observed in the isotropic or so-called fast-tumbling bicelle phase, over the range of temperatures investigated (10–40°C), for molar ratios of long-chain lipid to short-chain lipid between 0.20 and 1.0. Small angle neutron scattering data of this phase are consistent with the model in which bicelles were proposed to be disk-shaped. The experimentally determined dimensions are roughly consistent with the predictions of R.R. Vold and R.S. Prosser (*J. Magn. Reson. B* 113 (1996)). Differential paramagnetic shifts of head group resonances of dimyristoylphosphatidylcholine (DMPC) and dihexanoylphosphatidylcholine (DHPC), induced by the addition of Eu<sup>3+</sup>, are also consistent with the bicelle model in which DHPC is believed to be primarily sequestered to bicelle rims. Selective irradiation of the DHPC aliphatic methyl resonances results in no detectable magnetization transfer to the corresponding DMPC methyl resonances (and vice versa) in bicelles, which also suggests that DHPC and DMPC are largely sequestered in the bicelle. Finally, <sup>1</sup>H spectra of the antibacterial peptide indolicidin (ILPWKWPWWPWR-NH<sub>2</sub>) are compared, in a DPC micellar phase and the above fast-tumbling bicellar phases for a variety of compositions. The spectra exhibit adequate resolution and improved dispersion of amide and aromatic resonances in certain bicelle mixtures. © 2001 Elsevier Science B.V. All rights reserved.

**Keywords:** Bicelle; Membrane peptide; Model membrane; Nuclear magnetic resonance; Small angle neutron scattering; Indolicidin

### 1. Introduction

Due to stringent requirements for spectral resolution, high-resolution NMR studies of membrane proteins almost exclusively involve detergents or detergent mixtures, rather than more biologically mimetic membrane models. This frequently raises concerns

\* Corresponding author. Fax: +1-330-672-3816.

E-mail address: sprosser@membrane.kent.edu  
(R. Scott Prosser).

over protein misfolding and the degree to which enzymatic activity is preserved. Since a micelle typically contains 50–100 detergent molecules, serious concerns also arise regarding the small radius of curvature and the lack of a true lipid bilayer. Small unilamellar vesicles, which consist of single phospholipid bilayers, fare better as membrane models though their size and consequent 10–100-fold increase in rotational tumbling times (and line widths) prevent their application in conventional high-resolution NMR studies [13]. Recently, a new class of amphiphilic surfactants, referred to as amphipols, have been shown to readily solubilize membrane proteins in their native states [4,34]. Amphipols or amphipol–detergent mixtures may provide a better medium for some membrane proteins, from the perspective of resolution, if the aggregate size is smaller than in micelles. In rare circumstances, it may be possible to disregard the ‘rules’ and obtain three-dimensional structures of the native fold of membrane proteins, in a completely non-membrane mimetic environment, such as an organic solvent mixture [7].

Detergent micelles or micelle mixtures commonly consist of amphiphiles such as dodecylphosphocholine,  $\beta$ -D-octyl glucoside, or sodium dodecyl sulfate [35]. The detergent head groups may be designed to physically mimic the surface of a biological membrane. This may be useful in helping to promote the proper fold of many amphiphilic or surface associating membrane proteins. Moreover, a variety of water soluble peptides fold only upon addition of detergent [2,5]. Nevertheless, a variety of membrane peptides may require particular environments, in order to adopt their native fold. Antibacterial peptides represent one such example. Their specificity toward prokaryotic membranes is in many cases known to be related to physical properties such as the presence of negatively charged lipid, the presence of a transmembrane potential, or the influence of particular amphiphiles such as phosphatidylserine, cholesterol or phosphatidylethanolamine [9,10]. It is possible that a particular range of lipid compositions, unique to bacterial cells, give rise to a particular peptide structure and consequent antimicrobial activity. Therefore, it is desirable to employ a membrane mimetic, which reproduces many such features of bacterial membranes, in high-resolution (HR) NMR studies of antibacterial peptides. Fast-tum-

bling bicelles [37] are an ideal membrane mimetic in this regard<sup>1</sup>.

Bicelles have been enormously popular as model membrane systems for solid-state NMR [24,26–28]. A bicelle mixture, which consists of long-chain phospholipids, such as dimyristoylphosphatidylcholine (DMPC), and short-chain phospholipids, such as dihexanoylphosphatidylcholine (DHPC), in a molar ratio,  $q$ , between 2.8 and 5, adopts a magnetically alignable liquid crystalline phase, between approx. 37 and 45°C. This phase is known to consist of DMPC-rich bilayer domains, separated by DHPC defect regions. The observation that the <sup>31</sup>P and <sup>2</sup>H NMR spectra of the DHPC component of oriented bicelles are isotropic, prompted the model in which bicelles were proposed to consist of disk-shaped bilayer domains, whose edges were coated by a curved DHPC rim. The resulting disks were further hypothesized to adopt a nematic discoidal liquid crystalline phase. Though it is undisputed that magnetically aligned bicelles consist of long-chain lipid bilayers, their long range order or morphology has been brought into question with recent polarized microscopy measurements, in which the defect patterns of bicelles are revealed to be characteristic of a lamellar phase [31]. This is also supported by recent small angle neutron scattering (SANS) dilution measurements (i.e. dependence of average interparticle spacing with concentration) [17]. The lamellar liquid crystal consists of lipid bilayer domains, made predominantly from the long-chain phospholipid(s), and interspersed with DHPC defect regions. These defects may adopt a toroidal-like structure, within or between adjacent bilayers [21]. The magnetic anisotropy of the lipids is such that the average bilayer normal aligns perpendicular to the magnetic field [22,24]. This difference between the classic and current model of bicelle morphology is to some extent academic, since magnetically alignable bicelles remain as a useful model membrane system for studies of membrane peptides in aligned lipid bilayers.

Bicelles can also be adapted for HR NMR pur-

---

<sup>1</sup> Vold et al. [37] refer to bicelles for HR NMR purposes as isotropic bicelles. We use the term fast-tumbling bicelles, to avoid confusion with the word ‘isotropic’ and the bicelle shape.

poses. Vold et al. [37] demonstrated that for compositions,  $q$ , between 0.5 and 1.0, complete HR  $^1\text{H}$  NMR spectra of small membrane associated peptides such as mastoparan were observed. As in the original bicelle model, the fast-tumbling bicelles were also postulated to be disk-shaped. The motivation for the use of isotropic bicelles over micelles in NMR studies of membrane associated peptides is not only that the composition and conditions can be varied to better reproduce specific biological membranes, but that the bicelle interior consists of a true lipid bilayer, while DHPC is believed to be sequestered to the rim of the disks. Alternatively, DHPC and DMPC could simply adopt a mixed micellar phase, in which DHPC and DMPC are not truly sequestered. At issue in this paper are the morphology and dimensions of the fast-tumbling bicelles. Based on SANS and specific NMR experiments, this paper provides strong evidence that fast-tumbling bicelles consist of disk-shaped aggregates rather than mixed micelles. A similar finding regarding isotropic bicelles, in which the same conclusions are drawn from light-scattering, NMR, and fluorescence data, is being independently reported [8]. Together, these two studies validate the use of isotropic bicelles as membrane mimetic media for high-resolution NMR studies of membrane peptides.

## 2. Materials and methods

20% (w/w) bicellar dispersions consisting of phospholipid, 1,2-dimyristoyl-*sn*-glycero-3-phosphocholine (DMPC), 1,2-dimyristoyl-*sn*-glycero-3-phosphoglycerol (DMPG) and detergent, 1,2-dihexanoyl-*sn*-glycero-3-phosphocholine (DHPC), were prepared in 90.0%  $^2\text{H}_2\text{O}$  (Isotec, Miamisburg, OH) and 10%  $\text{H}_2\text{O}$ , and later diluted as needed. All lipids were obtained from Avanti Polar Lipids (Alabaster, AL) and used without further purification. A small amount of negatively charged lipid, DMPG, such as DMPC/DMPG = 20, was typically included in the bicelles [16]. In the paramagnetic shift experiments, DMPG also served to confine the majority of (positively charged) shift reagent to the presumed planar bilayer surface of the bicelles. Long-chain to short-chain lipid ratios (i.e. (DMPC+DMPG)/DHPC, referred to hereafter as  $q$ ) of 0.2, 0.5, and

1.0 were used. The samples were vortexed, followed by a few cycles of freeze thawing and centrifuging, after which a clear solution was obtained. Eu(III)-chloride hexahydrate (99.99%) was obtained from Aldrich Chemicals (Milwaukee, WI). After titrations, samples were mixed and allowed to equilibrate in the magnet for at least 20 min, before acquiring a spectrum.

Nuclear Overhauser effect spectroscopy (NOESY) and shift NMR experiments were performed on a Varian Inova 500 MHz high-resolution spectrometer, using the  $^1\text{H}$  channel of a 5 mm triple resonance inverse probe. One-dimensional spectra were acquired using a simple presaturation pulse of 1.5 s duration, applied to the water. Typically, 32–64 scans were obtained. All spectra were referenced to the aliphatic methyl DMPC peak which was defined to be 0.883 ppm, since the aliphatic DMPC methyl group should be least affected by the shift reagent. Homonuclear NOESY [15] spectra were obtained in a 95/5 ( $^2\text{H}_2\text{O}/\text{H}_2\text{O}$ ) mixture, using a recycle delay of 4 s, with 1024 data points in  $F_1$ , 2048 data points in  $F_2$ , and eight transients.

Unshifted fast-tumbling bicelle  $^1\text{H}$  NMR spectra were assigned by making use of the work of Hauser et al. [11] on DMPC in small unilamellar vesicles. DMPC and DHPC resonances in spectra in which  $\text{Eu}^{3+}$  shift reagent had been added, could be assigned by monitoring resonances through a careful progression of titrations, while two-dimensional NOESY spectra were used to confirm assignments and distinguish between DMPC and DHPC resonances.

Magnetization exchange experiments were performed on a Bruker 400 MHz DMX spectrometer by selectively saturating or inverting either the DHPC aliphatic or DMPC aliphatic resonances, using selective pulse lengths between 0.10 and 0.25 s, prior to the mixing period. A range of mixing (exchange) times from 0.001 to 9.0 s was used and a sufficient number of scans was acquired such that a 0.5% deflection in peak intensity through exchange could be detected.

Using a Bruker 4000 DMX and standard HNC inverse detect probe,  $^1\text{H}$  NMR WATERGATE spectra [20] off the membrane peptide, indolicidin (ILPWKWPWWPWR-NH<sub>2</sub>), were acquired in various 15–20% (w/w) micelle and bicelle, in which the solvent consisted of 95%  $\text{H}_2\text{O}/5\%$   $^2\text{H}_2\text{O}$ . The lipid/

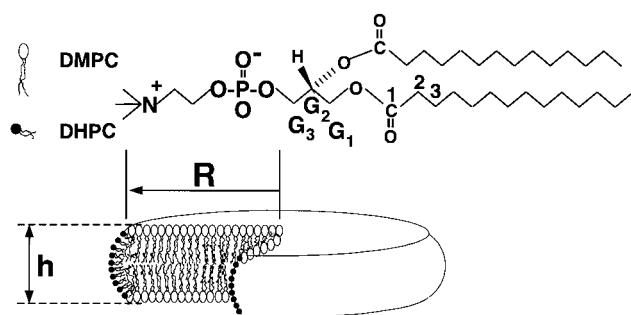


Fig. 1. The bicelle model, in which the disk-shaped bicelle consists of long-chain phospholipids (DMPC and DMPG), which predominately exist in the planar bilayer domain, and are coated by a rim of short-chain phospholipids (DHPC). *R* designates the bicelle disk radius, while *h* designates the total bilayer thickness (i.e. hydrophobic (*L*) plus hydrophilic (*2t*)).

peptide ratio or detergent/peptide ratio was approx. 50:1 and completely protonated lipids and detergents were used, with no attempt to selectively saturate the lipid or detergent resonances.

SANS scattering experiments were conducted using the NG3 and NG7 30 m instruments [6] at the Center of Neutron Research, located at the National Institute of Standards and Technology (Gaithersburg, MD). For most experiments, the wavelength ( $\lambda$ ) used was 5 Å, covering a *Q*-range between 0.004 Å<sup>-1</sup> and 0.3 Å<sup>-1</sup>, where *Q* is defined as  $(4\pi/\lambda) \sin(\theta/2)$ , and where  $\theta$  represents the angle between the incident and scattered beams. The two-dimensional raw data were corrected for dark current background (intrinsic to the detector) and empty cell scattering and put on an absolute scale (cross-section per unit volume) by a procedure that estimates neutron flux on the sample. The data were then circularly averaged to yield a one-dimensional intensity distribution, *I(Q)*.

### 3. Results and discussion

#### 3.1. The bicelle model: implications of size and morphology for high-resolution NMR studies

Fig. 1 depicts a bicelle, consisting of short- and long-chain phospholipids (i.e. DHPC and DMPC), and the appropriate nomenclature for specific protons. Typically, a small amount (5%) of negatively

charged long-chain lipids (DMPG) are incorporated as discussed above [32]. DMPG would be expected to be located primarily in the planar bilayer region with DMPC. As shown in Fig. 1, DMPC lipids predominate in a disk-shaped bilayer domain of radius *R*, which is coated with a DHPC rim of radius *h*/2. Assuming the DMPC and DHPC head groups occupy the same molecular cross-sectional areas, the molar ratio of long- to short-chain phospholipid may then be expressed as [36]

$$q = \frac{2\pi R^2}{\pi h[\pi R + h]} \quad (1)$$

This assumes that the lipids self-assemble and adopt a single morphology. Under the additional assumption that there is no phase separation, the above equation may be rearranged to give an expression which predicts the bicelle radius as a function of the molar ratio [36]

$$R = \frac{h}{4} q [\pi + (\pi^2 + 8/q)^{1/2}] \quad (2)$$

The dimensions are critically important for both achieving an aggregate size which is sufficiently small to be compatible with HR NMR resolution requirements, while at the same time maximizing the amount of bilayer lipid (DMPC and DMPG). Typically, molar ratios between  $q=0.5$  and  $q=1.0$  give acceptable <sup>1</sup>H spectral resolution for high-resolution NMR studies of small membrane peptides [37]. Detergent micelles, which are smaller than  $q=0.5$  bicelles, offer slightly better resolution at the cost of being less representative of a membrane. For micelles of radius *r* in a solvent of viscosity  $\eta$ , undergoing reorientational diffusion, a characteristic correlation time is given by [38]

$$\tau_c = \frac{4\pi\eta r^3}{3kT} \quad (3)$$

This expression would predict a correlation time of 14 ns at 40°C, for a micelle whose radius is 25 Å. In contrast, to describe the rotational diffusion of a bicelle, which may be approximated as a cylinder of radius *R* and thickness *h*, it is necessary to employ two correlation times,  $\tau_{\parallel}$  and  $\tau_{\perp}$ , associated with rotational diffusion about the cylinder axis and an orthogonal axis, such that the effective correlation time  $\tau_c$ , is given by

$$\tau_c = \left( \frac{1}{\tau_{\parallel}} + \frac{2}{\tau_{\perp}} \right)^{-1} \quad (4)$$

Though it is possible to derive the rotational correlation times for a given geometry, using hydrodynamic theory [33], the scaling of the effective correlation time with bicelle size can be approximated, using simple inertial arguments. Assuming a bilayer width of  $42 \pm 4 \text{ \AA}$ , determined from SANS fits (vide infra) we would predict bicellar radii ranging from  $21 \pm 3 \text{ \AA}$  for  $q=0.2$  bicelles, to  $43 \pm 4 \text{ \AA}$  for  $q=0.5$  bicelles and  $77 \pm 8 \text{ \AA}$  for  $q=1.0$  bicelles. The rotational correlation times,  $\tau_{\parallel}$  and  $\tau_{\perp}$ , should be proportional to the square roots of the respective moments of inertia of a disk (i.e.  $\sqrt{I_{\parallel}} = \sqrt{(m/2)R^2}$  and  $\sqrt{I_{\perp}} = \sqrt{(m/2)((R^2/2) + (2h^2/3))}$ ), where  $m$  represents the bicellar mass. Thus, at a constant temperature, the following proportionalities can be derived

$$\tau_c \propto \left( \frac{1}{R^2 h^{1/2}} + \frac{2}{R h^{1/2} \sqrt{\frac{R^2}{2} + \frac{2h^2}{3}}} \right)^{-1} \quad (5)$$

Using the above bicelle dimensions, we would thus expect the effective correlation time of the  $q=0.5$  and  $q=1.0$  bicelles to be respectively  $4\times$  and  $13\times$  that of the  $q=0.2$  bicelle. As will be shown, the spectral resolution available from a  $q=0.2$  sample of the antibacterial peptide, indolicidin, is comparable to that available from a micelle. Thus, there is a range of bicelle compositions which would be expected to furnish a bilayer-like environment, while giving rise to HR NMR spectra.

### 3.2. SANS

Small angle neutron scattering is extremely useful for elucidating morphologies of aggregates such as vesicles, micelles, and bicelles. SANS scattering curves are routinely measured with  $Q$ -ranges between  $0.004 \text{ \AA}^{-1}$  and  $0.3 \text{ \AA}^{-1}$ . The resultant patterns give information regarding intralamellar or interparticle spacing, typical bilayer widths, basic morphologies, and aggregate sizes or size distributions. Moreover, since deuterium and hydrogen have dramatically different scattering densities, it is possible to substitute deuterated lipids or detergents, to focus on scattering

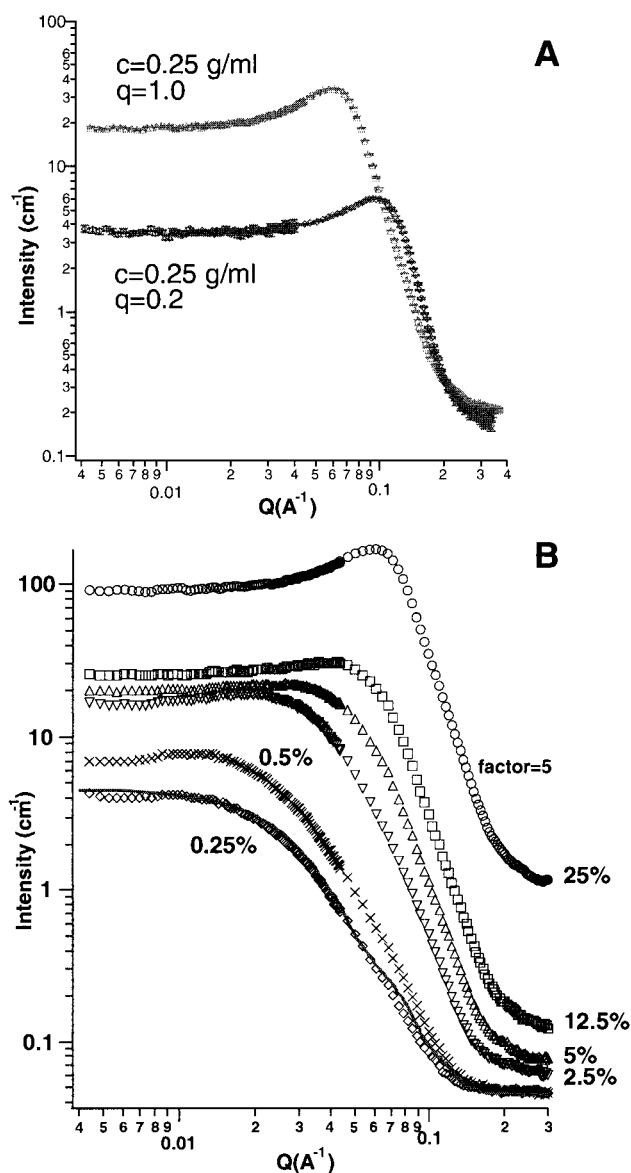


Fig. 2. (A) SANS profiles of  $q=1.0$ , and  $q=0.2$  bicelles at  $10^\circ\text{C}$  and 25% (w/w). In the most dilute case, both neutron scattering curves can be modeled by the bicelle (disk) model in which the bicelle is described by a planar bilayer radius,  $R$ , and a bilayer thickness,  $h$ . The fitted values of  $R$  are in good agreement with the predictions of Vold and Prosser [36]. The  $q=1.0$  and  $q=0.2$  samples exhibit a similar SANS profile at all temperatures investigated. (b) SANS profile of a  $q=1.0$  bicelle at  $10^\circ\text{C}$  and a range of concentrations (25–0.25% (w/w)). Note that the peak characterizing interparticle spacing is much less pronounced in the dilute bicelle mixture.

from a particular amphiphile or region of an aggregate such as a bicelle. It is also possible to prepare a mixture of  $\text{H}_2\text{O}$  and  $^2\text{H}_2\text{O}$  whose average scattering density matches the bilayer hydrophobic scattering

density, such that the SANS profile becomes sensitive to subtle structural features of the aggregate. The SANS profile,  $I(Q)$ , is typically modeled in terms of a form factor associated with the aggregate morphology (i.e. vesicle, micelle, bicelle, etc.). For example, a spherical shell model which has been used to describe the size (or distribution of sizes) of vesicles, in addition to bilayer widths, has been frequently invoked in SANS studies of vesicles [12]. Interparticle interactions also often affect the scattering functions, though in many cases this may be separated by monitoring scattering profiles as the sample is diluted, and using the most dilute SANS profile to determine the form factor.

The SANS profiles at 10°C for  $q=0.2$  and  $q=1.0$  fast-tumbling bicelles (25% w/w in 100%  $^2\text{H}_2\text{O}$ ) are shown in Fig. 2A. In each case, a low  $Q$  plateau is observed between approx. 0.004 and 0.04  $\text{\AA}^{-1}$ , with a prominent peak at 0.1  $\text{\AA}^{-1}$  and 0.06  $\text{\AA}^{-1}$  respectively, followed by a steep drop in the scattering intensity towards 0.2  $\text{\AA}^{-1}$ . The plateau confirms the absence of larger aggregates, and reveals the upper size limit of the bicelles. The SANS profile of a  $q=3.2$  sample (data not shown) is also observed to be consistent with the bicelle model at low temperatures. However, at higher temperatures, a distinct (non-bicellar) lamellar phase is observed in which aligned bilayers form at sufficient magnetic fields [17,31]. The prominent peak in each of the SANS profiles can be associated with a typical interparticle spacing,  $\xi_D = 2\pi/Q_{\text{peak}}$ . This interparticle spacing peak is gradually diminished as the sample is diluted and the scattering profile becomes representative of the single particle form factor, as shown for the 0.25% trace in Fig. 2B. It should be emphasized that the SANS profiles predicted by the spherical shell model for vesicles or micelles are dramatically different from the observed scattering profiles [12,17]. The possibility of polydisperse spheres was also considered using a variety of distributions; no suitable fit could be found. Finally, in the limited number of samples considered ( $q=0.2$ ,  $q=0.5$ , and  $q=1.0$ ) there was little variation in the SANS profiles with temperature, which suggests that the same approximate morphology of the fast-tumbling bicelles is maintained from 10°C to 40°C.

Using a simplified version of the bicelle model, in which the bicelle is imagined as a cylinder of radius

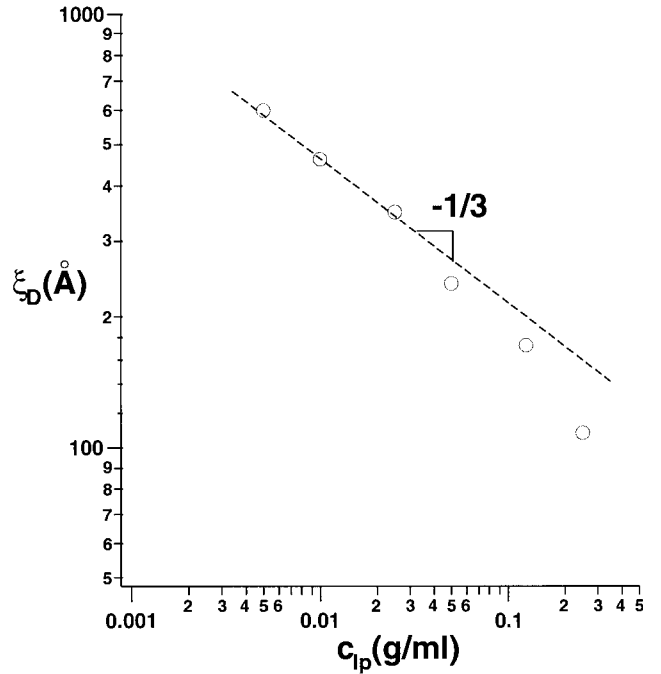


Fig. 3. Experimentally determined variation in the interparticle spacing,  $\xi_D$ , as a function of lipid concentration,  $c_{lp}$ , for a  $q=1.0$  bicelle mixture at 10°C.

$R$  and thickness  $h$ , the single particle form factor,  $P(Q)$ , which describes the SANS profiles at low concentrations, may be written as [17]

$$P(Q) = \frac{1}{V_{\text{lipid}}} \int_0^{\pi/2} g^2(Q, \alpha) \sin(\alpha) d\alpha \quad (6)$$

$$g(Q, \alpha) = 2(\rho_{\text{hydrophobic}} - \rho_{\text{hydrophilic}}) V_{\text{hydrophobic}}$$

$$\frac{\sin\left(\frac{QL}{2} \cos \alpha\right)}{\frac{QL}{2} \cos \alpha} \frac{J_1(QR \sin \alpha)}{QR \sin \alpha} +$$

$$2(\rho_{\text{hydrophilic}} - \rho_{\text{water}}) V_{\text{lipid}}$$

$$\frac{\sin(Q(R+t) \cos \alpha)}{Q(R+t) \cos \alpha} \frac{J_1(QR \sin \alpha)}{QR \sin \alpha} \quad (7)$$

where  $V_{\text{lipid}}$  and  $V_{\text{hydrophobic}}$  represent the respective volumes of the total bilayer lipid and the hydrophobic portion of the bilayer,  $\alpha$  represents the angle between the scattering vector,  $\mathbf{Q}$ , and the bilayer normal,  $\mathbf{n}$ , and  $J_1(x)$  is the first order Bessel function. Note that the above expression distinguishes an inner

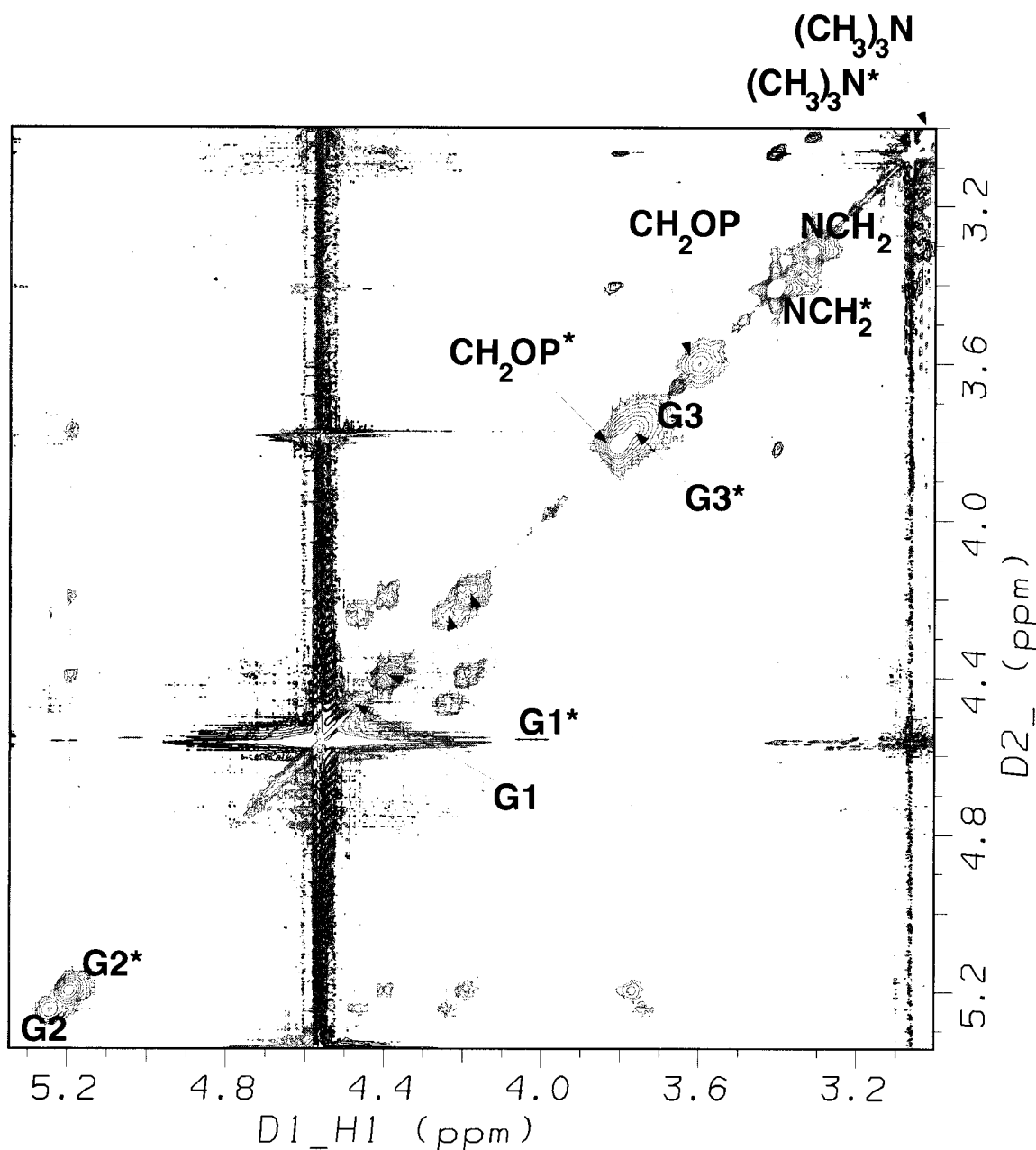


Fig. 4. Head group region of a 500 MHz  $^1\text{H}$  NMR NOESY spectrum (800 ms mixing time) at  $40^\circ\text{C}$  of a  $q=1.0$  bicelle, doped with  $\text{Eu}^{3+}$  shift reagent such that  $\text{DMPC}/\text{Eu}^{3+} \approx 30:1$ . The sample consisted of a 15% (w/w) aqueous mixture of DMPC, DHPC, and DMPG. The molar ratio of DMPC to DMPG was approx. 20 and  $q$  is defined as the molar ratio of long-chain phospholipid to short-chain phospholipid (i.e.  $q = (\text{DMPC} + \text{DMPG})/\text{DHPC}$ ).

hydrophobic layer of thickness,  $L$ , and two surrounding hydrophilic layers, of thickness,  $t$ , such that  $h = L + 2t$ . The free parameters in the consequent fit of the data involve scattering length densities and volumes ( $\rho_{\text{hydrophobic}}$ ,  $\rho_{\text{hydrophilic}}$ ,  $\rho_{\text{water}}$ ,  $V_{\text{lipid}}$ , and  $V_{\text{hydrophobic}}$ ) [17].  $\rho_{\text{hydrophobic}}$  and  $\rho_{\text{water}}$  can be pre-

cisely calculated, whereas  $\rho_{\text{hydrophilic}}$  is related to head group hydration and may be estimated from the literature; these parameters are held constant in the fitting. Additional parameters include those associated with the bicelle morphology, namely the bilayer disk radius,  $R$ , and the hydrophobic and hydro-

philic thicknesses,  $L$  and  $t$ . The parameters associated with thicknesses are also expected within a certain narrow range ( $30 \text{ \AA} < 50 \text{ \AA}$  and  $5 \text{ \AA} < t < 10 \text{ \AA}$ ). The result of the analysis gives an estimate of the bicelle dimensions (Table 1), which turn out to be very close to the values predicted by Vold and Prosser [36]. For example, for the  $q=1.0$  bicelle, the fitted parameter for the bicellar radius,  $R$ , is  $71.4 \pm 4 \text{ \AA}$ , at the lowest concentration, which compares favorably with the prediction of  $77 \pm 8 \text{ \AA}$ , using the formulae of Vold and Prosser [36]

The morphology of the bicelles can be further distinguished by monitoring the interparticle spacing,  $\xi_D$ , as a function of concentration,  $c_{lp}$ . The dependence of  $\xi_D$  with  $c_{lp}$  is indicative of the dimensionality of the liquid crystal mesogen. For example,  $\xi_D$  is typically inversely proportional to concentration (i.e.  $\xi_D \propto c_{lp}^{-1}$ ) for a (one-dimensional) lamellar phase, whereas a (three-dimensional) micellar or bicellar mixture should exhibit a dependence of  $c_{lp}^{-1/3}$ . As shown in Fig. 3, the power law approximately follows this ideal dependence. The slight deviation from ideality would be consistent with the formation of larger particles at lower concentrations. At concentrations below approx. 0.05 g/ml, a significant fraction of DHPC is known to be in exchange with solution [8], which would effectively result in a greater  $q$ , and thus particle size. No such deviations in the  $-1/3$  dependence of  $\xi_D$  with concentration of  $q=3.2$  bicelles at  $10^\circ\text{C}$  were observed.

### 3.3. High-resolution $^1\text{H}$ NMR

Through solid-state NMR, it is straightforward to differentiate between the orientational properties of

Table 1  
SANS fitting parameters for the most dilute  $q=1.0$  bicelle sample

Parameter	Value
$R$ ( $\text{\AA}$ )	$71.4 \pm 4$
$t$ ( $\text{\AA}$ )	$8 \pm 1$
$L$ ( $\text{\AA}$ )	$32 \pm 2$
$\rho_{\text{hydrophobic}}$ ( $\text{\AA}^{-2}$ )	$-4.3\text{e-}7$
$\rho_{\text{hydrophilic}}$ ( $\text{\AA}^{-2}$ )	$3.424\text{e-}6$
$\rho_{\text{water}}$ ( $\text{\AA}^{-2}$ )	$6.38\text{e-}6$
Incoh. bkg ( $\text{cm}^{-1}$ )	0.046

The scattering length densities were fixed in the fit.

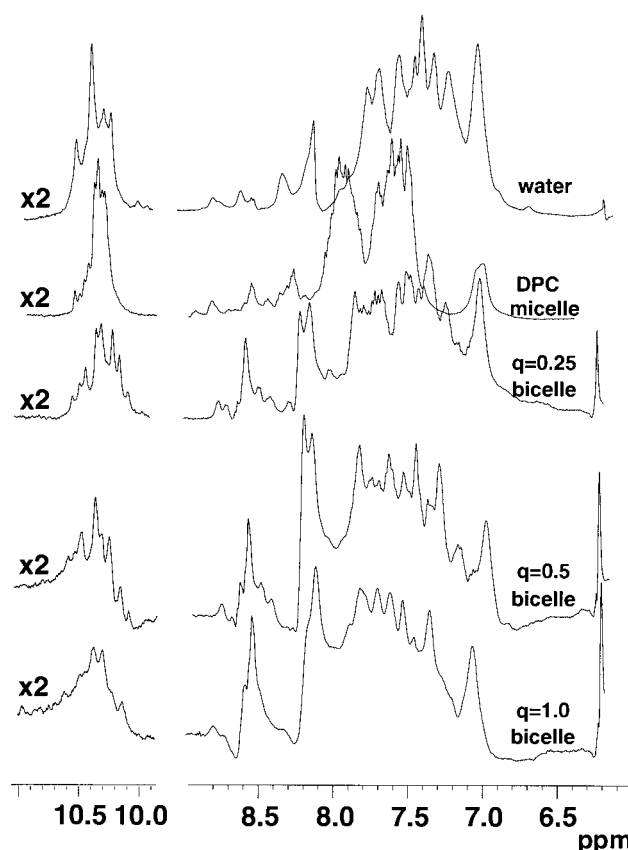


Fig. 5.  $^1\text{H}$  NMR WATERGATE spectra of the amide and aromatic region of indolicidin in fast-tumbling bicelles ( $q=0.25$ ,  $q=0.5$ , and  $q=1.0$ ), DPC micelles, and water. The water spectrum was obtained using 64 scans while the micelle and  $q=0.25$  bicelle samples required 512 scans and the  $q=0.5$  and  $q=1.0$  spectra were obtained using 1024 scans.

DHPC and DMPC and infer possible morphologies associated with magnetically aligned DMPC/DHPC mixtures. Early  $^{31}\text{P}$  and  $^2\text{H}$  NMR studies of bicellar mixtures helped delineate conditions under which bicellar mixtures formed an aligned bilayer phase (Sanders and Prestegard, 1990, [40]). Later studies [36] made use of both chain perdeuterated DHPC and DMPC to conclude that DHPC resided on a curved rim, while DMPC existed in a planar bilayer of a DMPC/DHPC aggregate, in keeping with the original bicelle model. HR  $^1\text{H}$  NMR spectra are much less informative in elucidating the possible morphology of bicellar mixtures in an isotropic phase<sup>2</sup>. At a given temperature, the  $^1\text{H}$  NMR spectra of DMPC and DHPC of the above fast-tumbling bicelles (i.e.  $q=0.2$  to  $q=1.0$ ) are very similar, with the exception of the aliphatic terminal methyl pro-



Table 2

Chemical shifts and Eu<sup>3+</sup>-induced shifts of  $q=0.5$  isotropic bicelles (DMPC/DMPG = 20, 40°C), in units of ppm

	(CH <sub>3</sub> ) <sub>3</sub> N	NCH <sub>2</sub>	CH <sub>2</sub> OP	G <sub>3</sub>	G <sub>2</sub>	G1 <sub>1</sub>	G1 <sub>2</sub>	C <sup>3</sup> H <sub>2</sub>	C <sup>N</sup> H <sub>2</sub>
Iso. bicelle+Eu <sup>3+</sup>	3.274	3.715	4.057	4.334	5.330	4.477	4.275	1.653	1.299
$\Delta\sigma$ (DHPC)	-0.210	-0.306	-0.249	-0.562	-0.133	-0.081	-0.085	-0.051	0.0
$\Delta\sigma$ (DMPC)	-0.252	-0.400	-0.458	-0.597	-0.087	-0.012	-0.036	-0.051	0.0

The mole ratio of DMPC to Eu<sup>3+</sup> was estimated to be 30:1.

tons. The above SANS data clearly reveal conditions under which isotropic bicelles are observed. Though spectroscopically equivalent (or nearly so), DMPC and DHPC are presumed to be sequestered in the bicelle model. Using lanthanide shift reagents, there are two ways in which differential paramagnetic shifts of DMPC and DHPC head group protons might be observed. The exposure of the head group protons to the shift reagent might be different for a small curved micellar surface or rim (DHPC) than that for the flat bilayer. Alternatively, if a small amount of negatively charged (DMPG) lipid is used in the bicellar mixture, the negatively charged lipid would be expected to homogeneously mix with DMPC in the planar bilayer region. Consequently, a slightly higher concentration of (positively charged) shift reagent might be observed in the bilayer region, resulting in greater pseudocontact shifts for DMPC head group peaks. On the other hand, if the DMPC/DMPG/DHPC mixture is simply a mixed micelle, we would expect the addition of shift reagent to result in paramagnetic shifts but with little or no differential shifting of the DMPC or DHPC resonances. As shown in the two-dimensional NOESY spectra in Fig. 4, the addition of Eu<sup>3+</sup> does indeed cause differential shifts of specific head group resonances. These shifts are similar to those originally observed by Hauser et al. [11] for a titration of Eu<sup>3+</sup> to a small unilamellar vesicle (SUV) mixture of dipalmitoylphosphatidylcholine, or DPPC. The paramagnetic shifts, which for lanthanides are primarily dipolar in origin, are given by [18,29]

$$\Delta\nu/\nu = W \frac{\beta^2 S(S+1)}{9kT} (g_{\parallel}^2 - g_{\perp}^2) \frac{1-3\cos^2\theta}{r_{\text{IS}}^3} \quad (8)$$

<sup>2</sup> We use the term isotropic throughout this paper, in the NMR context, meaning that the associated NMR spectra are purely isotropic.

where  $\beta = eh/2mc$ ,  $S$  is the spin of the paramagnetic species, and  $g_{\parallel}$  and  $g_{\perp}$  are familiar electronic  $g$ -tensor quantities.  $W$  is a function of the concentration and coordination number of the paramagnetic species, and  $r_{\text{IS}}$  represents the motionally averaged distance between the electronic and nuclear spins. Because the DMPC shifts are approximately proportional to those observed by Hauser et al. in SUVs, we conclude that the head group structure of DMPC in isotropic bicelles is similar to that in SUVs. Note that the choline, CH<sub>2</sub>N, and methylene resonances adjacent to the phosphate group all exhibit chemical shifts which are markedly different between DHPC and DMPC, upon addition of shift reagent. Careful titrations revealed the differential shift trend to be the same over a 20-fold range of Eu<sup>3+</sup> concentration (the NOESY spectrum represents the most (Eu<sup>3+</sup>) concentrated sample studied). Although lanthanides have been observed to alter lipid packing [1,39] at high concentrations (DMPC/Eu<sup>3+</sup>  $\approx$  5), we attribute the above differential shifts to the fact that DMPC and DHPC are sequestered to different regions of the bicelle, since these shifts are observed over a broad Eu<sup>3+</sup> concentration range.

Table 2 presents the lanthanide-induced shifts, for a DMPC/Eu<sup>3+</sup> mole ratio of roughly 30. Note in particular that the addition of Eu<sup>3+</sup> solution to the  $q=0.5$  bicelle results in (upfield) shifts of -0.252, -0.400, -0.458, and -0.597 ppm for the DMPC choline methyl, NCH<sub>2</sub>, CH<sub>2</sub>OP, and G<sub>3</sub> resonances respectively, as identified in Fig. 1. The comparative DHPC shifts at this concentration are -0.210, -0.306, -0.249 and -0.562 ppm. Thus, the majority of the DHPC shifts are smaller than the DMPC shifts. We observe a similar trend in the  $q=1.0$  bicelle, though resolution and consequent sensitivity in the NOESY experiment are somewhat compromised. These observations are consistent with the hypothesis that the  $q=1.0$  and  $q=0.5$  systems are bicelles and that the local concentration of the Eu<sup>3+</sup> is higher in

the planar DMPC/DMPG region due to the presence of additional negatively charged lipid or possibly due to the difference in the radius of curvature of the planar region and the rim. Thus, the lanthanide-induced DMPC shifts are greater than the DHPC shifts. The differences in DMPC and DHPC shifts are also consistently larger in the  $q=1.0$  isotropic bicelle sample than in the  $q=0.5$  bicelle. We interpret this to mean that the DMPC and DHPC amphiphiles are more separated in the  $q=1.0$  sample, and occupy two distinct environments. It is possible that there is a greater degree of lipid exchange between the planar bilayer region and rim in the  $q=0.5$  bicelle. As a control, we measured similar spectra of DHPC alone as a function of  $\text{Eu}^{3+}$  concentration. In this case, none of the assigned  $^1\text{H}$  resonances were observed to split into two or more resonances, upon addition of  $\text{Eu}^{3+}$ . High-resolution  $^1\text{H}$  NMR can also determine the degree of demixing or the degree to which DMPC and DHPC are sequestered in the bicelle. One such experiment involves selective saturation or inversion of the aliphatic methyl peak of DHPC, followed by a mixing time ( $\tau_m$ ) and subsequent measurement of the entire spectrum, to detect  $\tau_m$ -dependent changes in peak height of the aliphatic methyl peak of DMPC (and vice versa). Such changes would arise from DHPC–DMPC cross-relaxation and would be expected to be prominent in a completely mixed aggregate (mixed micelle) with nearly equimolar constituents. Cross-relaxation should be much less pronounced in a demixed aggregate such as a bicelle. Huster et al. [14] have previously studied cross-relaxation phenomena in membranes between spectroscopically inequivalent DMPC resonances. A careful series of  $\tau_m$ -dependent NOESY experiments on DMPC vesicles, under magic-angle spinning, revealed significant cross-relaxation. By employing different fractions of perdeuterated DMPC, the authors were able to determine that the bulk of lipid cross-relaxation arose from intermolecular contact rather than spin diffusion. In our case, we made use of the two spectroscopically inequivalent aliphatic methyl peaks (DHPC and DMPC) to assess cross-relaxation and the degree of demixing. The analysis of such selective saturation or inversion experiments can be easily described by the Bloch equations and are described using two coupled differential equations, which are parameterized by two independent ex-

change rates, and the respective spin-lattice relaxation times of DHPC and DMPC methyl groups [3].

The above cross-relaxation process is most easily studied by a different NOE experiment. Rather than selectively saturate a resonance, we utilized a selective  $\pi$  pulse applied to the aliphatic methyl DHPC resonance in one case and the corresponding DMPC resonance in the second case. Using mixing times,  $\tau_m$ , ranging from 0.5 ms to 9 s, and a sufficient number of scans to reliably detect as little as a 0.5% change in the DMPC methyl peak, no cross-relaxation was observed in a  $q=1.0$  bicelle at 40°C (i.e. no change in the intensity of the unperturbed methyl resonance as a function of mixing time). This also proved to be the case when the methyl DMPC resonance was selectively irradiated. These experiments further validate the bicelle model in which DMPC and DHPC are proposed to be sequestered.

Lastly, to truly assess spectral resolution, it is important to compare HR  $^1\text{H}$  NMR spectra of a membrane peptide in micelles and the fast-tumbling bicelles. The antibacterial peptide, indolicidin, whose sequence is ILPWKWPWWPWR-NH<sub>2</sub>, is the perfect candidate for such studies. Indolicidin is the smallest of the known naturally occurring linear antimicrobial peptides and is known to permeabilize the outer membrane of Gram-negative bacteria by self-promoted uptake [19] and is active against Gram-positive bacteria, fungi, protozoa, and recently, HIV-1 [30]. The structure of indolicidin has recently been determined in DPC and SDS micelles [25]. This HR NMR study revealed that the backbone structure in DPC, which is well defined between residues 3 and 11, is extended, with two half-turns at residues Lys-5 and Trp-8. The peptide has a central hydrophobic core and is bracketed by positively charged regions near the peptide termini. The peptide was observed to adopt a wedge shape, with Trp-8 most deeply buried in the membrane [23]. At lipid/peptide ratios of approx. 50 or more, indolicidin is found to be fully bound and immersed into the bicelle or micelle [25]. Therefore, under the conditions of the experiments in this study, no additional motional averaging of indolicidin would be expected from exchange on and off the surface. Fig. 5 shows the amide and aromatic regions of the  $^1\text{H}$  NMR spectra of indolicidin in water, DPC micelles and three fast-tumbling bicelle systems. The bicelle spectra are sim-

ilar to the micelle spectrum though all three ( $q = 0.25$ ,  $q = 0.5$ , and  $q = 1.0$ ) exhibit improved dispersion, particularly in the amide region. Greater dispersion would be expected for a well-formed helix, particularly if a portion of the peptide was more deeply immersed in the membrane, while the remainder was exposed to the water interface. Clearly the  $q = 0.25$  and  $q = 0.5$  bicelles give acceptable resolution, whereas one might consider using the  $q = 1.0$  bicelle in combination with  $^{13}\text{N}$ - or  $^{15}\text{N}$ -labeled peptides. Note that the baseline distortions in the  $q = 0.5$  and  $q = 1.0$  bicelles simply arise from the overwhelming lipid signal which was not attenuated in these experiments.

#### 4. Conclusions

The isotropic bicelles are an ideal model system for high-resolution NMR studies of membrane peptides. Their particular advantages include the fact that the bicelle size (i.e.  $R$ ) can be controlled by varying the molar ratio,  $q$ , of long-chain phospholipid (DMPC and DMPG) to short-chain phospholipid (DHPC). SANS data show that between compositions of  $q = 0.2$  and  $q = 1.0$  and temperatures of  $T = 10^\circ\text{C}$  and  $40^\circ\text{C}$ , bicelle mixtures adopt the idealized disk-shaped morphologies, in which the planar bilayer radius,  $R$ , ranges from 21 Å ( $q = 0.2$ ) to 77 Å ( $q = 1.0$ ). The bicelle model is also consistent with SANS measurements of  $q = 3$  bicelle mixtures at low temperatures only ( $10^\circ\text{C}$ ). Dilution experiments, in which the interparticle spacing is measured by SANS as the bicelle mixtures are diluted, further validate the bicelle model.

HR  $^1\text{H}$  NMR experiments reveal that although DMPC and DHPC resonances are identical, with the exception of the aliphatic methyl resonances, the addition of paramagnetic shift reagent,  $\text{Eu}^{3+}$ , causes substantial differential shifts of DMPC and DHPC head group resonances. In the presence of a small amount of DMPG, the largest shifts are observed with the DMPC resonances. This effect is attributed to the fact that DMPC and DHPC are sequestered in separate environments, consistent with the bicelle model. The bicelle model is further tested by an exchange experiment in which one methyl resonance is selectively inverted, while cross-relaxation

is monitored to the other methyl resonance during a mixing time,  $\tau_m$ . No cross-relaxation was observed for a large range of mixing times, in the  $q = 1.0$  bicellar mixture at  $40^\circ\text{C}$ , implying that DMPC and DHPC are primarily demixed, or sequestered, as proposed in the bicelle model. These experiments could be extended by exploring cross-relaxation effects after addition of shift reagents, in which case DHPC and DMPC could be easily discriminated. Finally, HR  $^1\text{H}$  NMR of the peptide indolicidin in  $q = 0.25$  and  $q = 0.5$  bicelles reveals excellent resolution and dispersion, in comparison with spectra obtained in micelles.

Additional SANS experiments are underway to map out the complete morphology of bicelles under conditions of temperature and a variety of compositions. These measurements will be made in parallel with NMR studies assessing spectral resolution in membrane peptide studies.

#### Acknowledgements

R.S.P. gratefully acknowledges Research Corporation (RI0322) and the Liquid Crystal Institute at Kent State University. We also thank the Nucleic Acids Protein Services (NAPS) unit at UBC for synthesizing the indolicidin peptide analogues.

#### References

- [1] H. Akutsu, J. Seelig, *Biochemistry* 20 (1981) 7366–7373.
- [2] W. Braun, G. Wider, K.H. Lee, K. Wüthrich, *J. Mol. Biol.* 169 (1983) 921–948.
- [3] A.P. Campbell, B.D. Sykes, *J. Magn. Reson.* 93 (1991) 77–92.
- [4] P. Champeil, T. Menguy, C. Tribet, J.L. Popot, M. le Maire, *J. Biol. Chem.* 275 (2000) 18623–18637.
- [5] H.J. Dyson, P.E. Wright, *Annu. Rev. Biophys. Biophys. Chem.* 20 (1991) 519–538.
- [6] C.J. Glinka, J.G. Barker, B. Hammouda, S. Krueger, J.J. Moyer, W.J. Orts, *J. Appl. Crystallogr.* 31 (1998) 430–445.
- [7] M.E. Girvin, V.K. Rastogi, F. Abildgaard, J.L. Markley, R.H. Fillingame, *Biochemistry* 37 (1998) 8817–8824.
- [8] K.J. Glover, J.A. Whiles, G. Wu, N. Yu, R. Deems, J.O. Struppe, R. Stark, E.A. Komives, R.R. Vold, *Biophys. J.* (2001) submitted.
- [9] R.E.W. Hancock, *Lancet* 349 (1997) 418–422.
- [10] R.E.W. Hancock, D.S. Chaplin, *Antimicrob. Agents Chemother.* 43 (1999) 1317–1323.

- [11] H. Hauser, W. Guyer, I. Pascher, P. Skrabal, S. Sundell, *Biochemistry* 19 (1980) 366–373.
- [12] J.B. Hayter, in: V. Degiorgio, M. Corti (Eds.), *Physics of Amphiphiles*, Elsevier, Amsterdam, 1985.
- [13] G.D. Henry, B.D. Sykes, *Methods Enzymol.* 239 (1994) 515–535.
- [14] D. Huster, K. Arnold, K. Gawrisch, *J. Phys. Chem. B* 103 (1999) 243–251.
- [15] J. Jeener, B.H. Meier, P. Bachmann, R.R. Ernst, *J. Chem. Phys.* 71 (1979) 4546–4553.
- [16] J.A. Losonczi, J.H. Prestegard, *J. Biomol. NMR* 12 (1998) 447–451.
- [17] M.P. Nieh, C.J. Glinka, S. Krueger, R.S. Prosser, J. Katsaras, *Langmuir* (2001) in press.
- [18] J.A. Peters, J. Huskens, D.J. Raber, *Prog. NMR Spectrosc.* 28 (1996) 283–350.
- [19] K.L. Piers, M.H. Brown, R.E.W. Hancock, *Antimicrob. Agents Chemother.* 38 (1994) 2311–2316.
- [20] M. Piotto, V. Saudek, V. Sklenar, *J. Biomol. NMR* 2 (1992) 661–665.
- [21] R.S. Prosser, V.B. Volkov, I.V. Shiyankovskaya, *Biochem. Cell Biol.* 76 (1998) 443–451.
- [22] R.S. Prosser, I.V. Shiyankovskaya, *Concepts Magn. Reson.* 13 (2001) 19–31.
- [23] R.S. Prosser, P.A. Luchette, P.W. Westerman, A. Rozek, R.E.W. Hancock, *Biophys. J.* (2001) in press.
- [24] P. Ram, J.H. Prestegard, *Biochim. Biophys. Acta* 940 (1988) 289–294.
- [25] A. Rozek, C.L. Friedrich, R.E.W. Hancock, *Biochemistry* 39 (2000) 15765–15774.
- [26] C.R. Sanders, J.P. Schwonek, *Biochemistry* 31 (1992) 8898–8905.
- [27] C.R. Sanders, B.J. Hare, K.P. Howard, J.H. Prestegard, *Prog. NMR Spectrosc.* 26 (1994) 421–444.
- [28] C.R. Sanders, R.S. Prosser, *Structure* 6 (1998) 1227–1234.
- [29] J.D. Saterlee, *Concepts Magn. Reson.* 2 (1990) 69–79.
- [30] M.E. Selsted, M.J. Novotny, W.L. Morris, Y.Q. Tang, W. Smith, J.S. Cullor, *J. Biol. Chem.* 267 (1992) 4292–4295.
- [31] I.V. Shiyankovskaya, O.D. Lavrentovich, R.S. Prosser, (2001) manuscript in preparation.
- [32] J. Struppe, J.A. Whiles, R.R. Vold, *Biophys. J.* 78 (2000) 281–289.
- [33] M.M. Tirado, J.G. de la Torre, *J. Chem. Phys.* 73 (1980) 1986–1993.
- [34] C. Tribet, R. Audebert, J.L. Popot, *Proc. Natl. Acad. Sci. USA* 93 (1996) 15047–15050.
- [35] O. Vinogradova, F. Sonnichsen, C.R. Sanders, *J. Biol. NMR* 11 (1998) 381–386.
- [36] R.R. Vold, R.S. Prosser, *J. Magn. Reson. B* 113 (1996) 267–271.
- [37] R.R. Vold, A.J. Deese, R.S. Prosser, *J. Biomol. NMR* 9 (1997) 329–335.
- [38] K. Wüthrich, *NMR of Proteins and Nucleic Acids*, Wiley, New York, 1986.
- [39] C.B. Yuan, D.Q. Zhao, B. Zhao, Y.J. Wu, J.H. Liu, J.Z. Ni, *Langmuir* 12 (1996) 5375–5378.
- [40] C.R. Sanders, J.H. Prestegard, *Biophys. J.* 12 (1990) 447–460.